Archival Report

Biological Psychiatry: GOS

Astrogliosis Occurs Selectively in Amygdala of Adolescent Primate and Rodent Following Daily Δ^9-Tetrahydrocannabinol, Prevented by Cannabidiol Co-Treatment

Yalin Sun, Meenalochani Sivasubramanian, Marija Milenkovic, Andrew Gumbert, Jack Bergman, Preston Ge, Myriam Heiman, Marie-Eve Di Raddo, Sarah L. Withey, Bertha K. Madras, and Susan R. George

ABSTRACT

BACKGROUND: Adolescent-onset cannabis use confers higher risk for neuropsychiatric disorders, implicating amygdala dysfunction. However, the mechanisms that mediate Δ^9-tetrahydrocannabinol (THC)–triggered neuroadaptive changes in the maturing amygdala remain unclear.

METHODS: Proteomic analysis of amygdala tissue from male adolescent *Saimiri boliviensis* nonhuman primates chronically treated with THC provided leads for targeted analyses of glial fibrillary acidic protein (GFAP), stathmin-1, and neuronal cell adhesion molecule (NrCAM) in a second species of male adolescent (postnatal day [P]35) and adult (P70) Sprague-Dawley rats. Primate activity monitoring and rat behavioral testing revealed THC-disrupted sleep architecture and anxiety-related behavior, respectively. Primary rat astrocyte cultures provided mechanistic insight into THC activation of astrocyte inflammatory function.

RESULTS: THC-induced upregulation of GFAP and complement factor-B (CF-B) signified proinflammatory glial activation exclusively in the adolescent amygdala, an effect absent in other brain regions and in adults. THC attenuated synaptic plasticity enhancers, stathmin-1 and NrCAM, effects not recapitulated in adults. Co-administered cannabidiol (CBD) prevented astrogliosis but did not restore synaptic plasticity marker levels. Astrogliosis was correlated with fragmented sleep, and attenuated plasticity markers were correlated with anxiety. THC-induced GFAP and CF-B upregulation with attenuation by CBD were replicated in cultured astrocytes, requiring cannabinoid type 1 receptor (CB1R)-activated calcium signaling. Elevated CB1R expression in the maturing brain was astrocyte-localized in the amygdala, but neuronal in the cortex and striatum.

CONCLUSIONS: Brain region- and age-specific regulation of CB1R in astrocytes critically links THC and unique adolescent amygdala vulnerability to inflammatory gliosis, impairing behaviors implicated in neuropsychiatric disorders. Mitigation of specific THC-induced changes by CBD offers leads for attenuating some adverse effects of THC.

https://doi.org/10.1016/j.bpsgos.2025.100496

Increased cannabis use has been observed with growing legalization and commercialization facilitating new cannabis consumption trends, such as greater incidence of daily use and use of higher potency forms of cannabis or its main psychoactive component, Δ^9-tetrahydrocannabinol (THC) (1). The magnitude and persistence of adverse cannabis-related consequences are associated with dose, use frequency, duration of use, and age of use onset (2,3). Compared to adult-onset use, evidence has revealed divergent neurochemical changes imparted by adolescent-onset cannabis use, which confers a heightened risk of developing psychiatric disorders (4–8).

Vulnerability to cannabinoids during the critical adolescent neurodevelopment period is foreseeable (9,10), as the endocannabinoid system continues to mature and contributes to shaping brain circuitry (11–13). By competing with endocannabinoids or activating the cannabinoid type 1 receptor (CB1R), THC triggers incompletely understood neuroadaptive changes.

Cannabinoids affect multiple brain regions that express relatively high levels of endocannabinoid system components, including the amygdala (14). Functionally, the amygdala biases behavioral outputs enhancing survival by registering and propagating sensory cues that indicate resources, threats, fear, or safety to process fearful or rewarding stimuli (15–18). Dysfunction of the amygdala has been implicated in psychiatric symptoms and disorders associated with adolescent cannabis use, including anxiety, depression, psychosis, and hypersensitivity to threat (19–22).

ISSN: 2667-1743

We sought to determine hallmarks of amygdala dysregulation in nonhuman primate and rodent models following prolonged, repeated, low-dose THC exposure in adolescence using a top-down, unbiased cellular transcriptome and proteome profiling analysis approach, with results highlighting the critical role that astrocytes in the amygdala play in the sensitivity of adolescents to cannabis exposure.

METHODS AND MATERIALS

For detailed materials and methods information, see the Supplement.

Animals

Adolescent and Adult Nonhuman Primates. Adolescent (2–2.5 years) drug- and experiment-naïve male squirrel monkeys (*Saimiri boliviensis*) and adult rhesus macaque monkeys (*Macaca mulatta*; see the Supplement for specific administration protocol) were used for chronic THC/THC+cannabidiol (CBD) administration primate studies.

Weekly intramuscular injections of THC and/or CBD doses in adolescents were progressively increased over a 3-week period to the daily administration dose of vehicle, 1 mg/kg THC or 1 mg/kg THC + 3 mg/kg CBD, as previously described (23). The dose of THC was chosen based on THC content in a standard cannabis joint containing 20% to 24% THC (60–72 mg THC), which translates to approximately 1 mg/kg for a 70 kg person (24,25). The dose of CBD was chosen based on effective ranges that ameliorate THC-induced anxiogenic and cognition-impairing effects in human and nonhuman primate subjects (26–28). The dose of CBD was also selected based on the initial therapeutic 2.5 mg/kg CBD dose of a cannabidiol anti-epileptic in a pediatric population (29).

Subjects were anesthetized with a mixture of ketamine, phenytoin, and pentobarbital 24 hours after the last drug injection, which was rapidly followed by brain dissection. Anatomically matched left hemisphere regions were snap-frozen, and the right hemispheres were postfixed.

Rats. Adult (postnatal day [P]70) and adolescent (P35) male Sprague-Dawley rats underwent 28 days of daily intraperitoneal injections of vehicle, 1 mg/kg THC, or 1 mg/kg THC + 3 mg/kg CBD between 10 AM and 12 PM. THC and CBD doses were selected by similar principles as those in nonhuman primates, with 1 mg/kg THC and 3 mg/kg CBD reaching similar blood concentrations in rats as those observed in human cannabis users (30–32). Animals were euthanized 1 hour after the final drug injection with CO_2 overdose and decapitation. Whole brains were dissected and snap-frozen in isopentane.

Behavioral Analyses

Sleep Monitoring: Adolescent Nonhuman Primates. Activity was monitored 24 hours a day using Fitbit Wireless Activity Trackers (Fitbit Zip), which were secured in an inaccessible custom-designed jacket. Data were collected daily and averaged for 3-week periods. Nighttime fragmented activity was defined as total activity counts after at least 1 hour with 0 activity counts. Subsequent activity that occurred between the last hour of inactivity and before light illumination was counted.

Rat Behaviors. For all rat behavioral testing, animals were administered their daily drug or vehicle injection 30 minutes prior to testing. Subjects were placed in the dark compartment of a light-dark box and in the center of the elevated plus maze and behaviors were manually or automatically recorded for over 5 minutes. For novelty-induced hypophagia, subjects trained to consume sweetened condensed milk were placed in an anxiogenic environment for latency and volume of consumption measurements.

Immunohistochemistry and In Situ Hybridization

Immunohistochemistry was performed in 3 independent laboratories using slightly modified protocols: 1) McLean Hospital (postfixed primate amygdala of right hemisphere: GFAP [glial fibrillary acidic protein]); 2) Massachusetts Institute of Technology (postfixed primate amygdala of right hemisphere: GFAP, CB1R, S100β); 3) University of Toronto (fresh frozen left hemisphere brain; primate amygdala: proteomics, GFAP, complement factor-B [CF-B], stathmin-1, NeuN, CB1R; prefrontal cortex [PFC] and caudate nucleus [CN]; rat brain).

Protocols were similarly conducted, with sections permeabilized, blocked, and incubated with primary antibodies at 4 °C overnight. Tissues were then incubated with fluorescent secondary antibodies and mounted with DAPI. Fluorescent in situ hybridization in drug-naïve P35 and P70 rat brain was performed for *Cnr1*, *Gfap*, and *Rbfox3* messenger RNAs (mRNAs) according to manufacturer's instructions.

In Vitro Primary Culture Experiments

Primary Rat Astrocyte Culture. Cortex, striatum, and hippocampus from P1 to P2 rat pups were triturated in astrocyte complete medium for seeding in T75 flasks and maintained at 37 °C, 5% CO_2 with humidity. On day in vitro 7, astrocytes were reseeded in 96-well plates for calcium measurements or poly-D-lysine-coated glass coverslips for immunofluorescence.

Primary Astrocyte Drug Treatments. THC and CBD were provided by Cannascribe and the National Institutes of Health (National Institute on Drug Abuse drug supply program). THC, CBD, BAPTA-AM, and rimonabant were dissolved in ethanol or DMSO. Inhibitors were added 1 hour or 10 minutes before THC.

For calcium measurements, all drugs were diluted in DMSO and Ringer's solution. Baseline readings with rimonabant, YM-254890, and 2-aminoethoxydiphenylborate (2-APB) were taken prior to THC-stimulated readings.

Statistical Analysis

All data were graphed and analyzed using GraphPad Prism 9.0 (GraphPad Software) as the average value ± SEM from at least 3 independent experiments. Statistical details are reported in each figure legend.

RESULTS

Adolescent but Not Adult Exposure to THC Induces a Proinflammatory Reactive Astrocyte Phenotype in the Nonhuman Primate Amygdala

Proteomic analysis of left hemisphere amygdala from young, male adolescent *Saimiri boliviensis* monkeys treated daily for 4 months with vehicle, THC, or THC+CBD (Figure 1A) revealed that THC significantly upregulated GFAP, an astrocytic cytoskeletal filament protein (Figure 1A and Figure S1). In contrast, THC conferred downregulation of stathmin-1, a neuronal protein with microtubule-destabilizing functions to enhance plasticity (33,34). Similarly, THC caused downregulation of neuronal cell adhesion molecule (NrCAM), a protein that is expressed by both neurons and astrocytes with functions of enhancing tripartite synapse stability via transcellular interactions (35,36). Co-administration of THC with CBD reversed GFAP upregulation but did not attenuate stathmin-1 and NrCAM downregulation. Gene expression profiles of left hemisphere amygdala from the same adolescent primates revealed discordant protein-RNA expression patterns, with GFAP, stathmin-1, and NrCAM protein levels not paralleled by comparable changes in RNA (Figure S2A).

Proteomics findings were validated by immunohistochemistry of left hemisphere amygdala of adolescent monkeys (Figure 1C, D), confirming GFAP upregulation in THC-treated compared with control or THC+CBD-treated subjects. Since astrocyte reactivity confers increased GFAP and possible inflammatory changes (37), another indicator of inflammatory response, CF-B, was evaluated. CF-B was also upregulated by THC, but not if THC and CBD were co-administered (Figure 1E). As increased glial proliferation accompanies astrocyte reactivity (38), the proportion of GFAP+ astrocytes as a fraction of total cell density was quantified. Astrocyte density was increased in THC-treated subjects and was reversed by CBD co-administration (Figure 1F), with astrocyte density positively correlated with CF-B and GFAP levels (Figure 1G).

Right hemisphere amygdala from the same subjects was analyzed by 2 other independent laboratories as a secondary validation measure for GFAP, in addition to astrocytic protein S100β and CB1R. GFAP was elevated in both the basolateral amygdala (BLA) and central amygdala nuclei of THC-treated adolescent monkeys (Figure 1H and Figure S2B, C). Daily THC reduced CB1R, elevated GFAP and the number of S100β-positive cells in the right basal amygdala nucleus of adolescent primates (Figure 1I–L and Figure S3A). CB1R was detected on astrocytes of all 3 treatment groups (Figure 1I). GFAP elevation was again prevented by CBD co-treatment and was positively correlated with the number of S100β-positive cells (Figure 1M). The regulator of neuronal plasticity stathmin-1 identified by proteomic analysis decreased by 51.34% ± 28.77% in THC-treated adolescent amygdala, but CBD co-administration did not modify the decrease (Figure 1N, O).

GFAP expression was analyzed in left hemisphere PFC and CN of THC-treated adolescent primates, with no detectable changes in either brain region (Figure 1P–R). To determine whether reactive astrogliosis in amygdala occurred following adult-onset THC exposure, amygdala GFAP expression was measured in a separate cohort of adult rhesus monkeys treated with a similar but shorter treatment duration. Adult squirrel monkeys were not available at the time of this study. GFAP was not elevated in adult rhesus primate amygdala following THC or THC+CBD treatment (Figure 1S, T), possibly suggesting that THC-induced astrogliosis may be specific to adolescent amygdala. However, the use of a different species for the analysis of THC effects in adult nonhuman primate amygdala required further controlled investigation within the same species. In summary, GFAP was upregulated by daily THC, blocked by co-administration with CBD, and observed exclusively in the left and right amygdala of adolescent nonhuman primates but not in the PFC or CN.

Adolescent-Specific Reactive Astrogliosis and Downregulated Neuronal Plasticity-Related Proteins Stathmin-1 and NrCAM Following THC Are Replicated in Rat Amygdala

These findings in nonhuman primates warranted confirmation, particularly to better control for species and treatment duration. In a species-appropriate scaled treatment paradigm, male adolescent (P35) and adult (P70) Sprague-Dawley rats were treated daily in parallel with vehicle, THC, or THC+CBD for 28 days (Figure 2A). In amygdala of adolescent rats treated with THC starting on P35, GFAP and CF-B expression were elevated, but not if CBD was co-administered (Figure 2B, C, E). Amygdala of adult rats treated with THC or THC+CBD starting on P70 showed no change in GFAP or CF-B (Figure 2B, D, F). Daily THC exposure decreased stathmin-1 and NrCAM expression in adolescent but not adult rat amygdala (Figure 2G, H, J–L), with downregulated NrCAM incompletely reversed by CBD in adolescents. These changes were not due to basal age differences in stathmin-1 and NrCAM expression because drug-naïve P35/P70 rats exhibited similar expression levels in amygdala (Figure S2A). Although classically characterized as neuronal proteins, the possibility of astrocytic expression of both proteins was investigated given the predominant changes in astrocytes following adolescent THC exposure. A subpopulation of rat astrocytes in primary culture was stathmin-1- or NrCAM-positive (Figure S3B), suggesting that their altered expression in vivo may be of glial or neuronal origin. These results revealed that THC elicited robust age-dependent changes specific to the adolescent amygdala, with proinflammatory astrogliosis and reduced expression of stathmin-1 and NrCAM.

Inflammation and Glial Dysfunction Correlated With Sleep Fragmentation Whereas Altered Neuronal Plasticity Proteins Correlated With Anxiety- and Anhedonic-Like Behaviors in Adolescents Chronically Exposed to THC

Throughout THC treatment of adolescent primates, activity monitoring (39) revealed trends for increased sleep fragmentation over time in THC-treated subjects (Figure 3A, B). Levels of GFAP, CF-B, and astrocyte numbers were correlated with the degree of sleep fragmentation quantified in each subject.

In the first sampling epoch (weeks 1–3 of drug administration), only GFAP levels and sleep fragmentation were positively

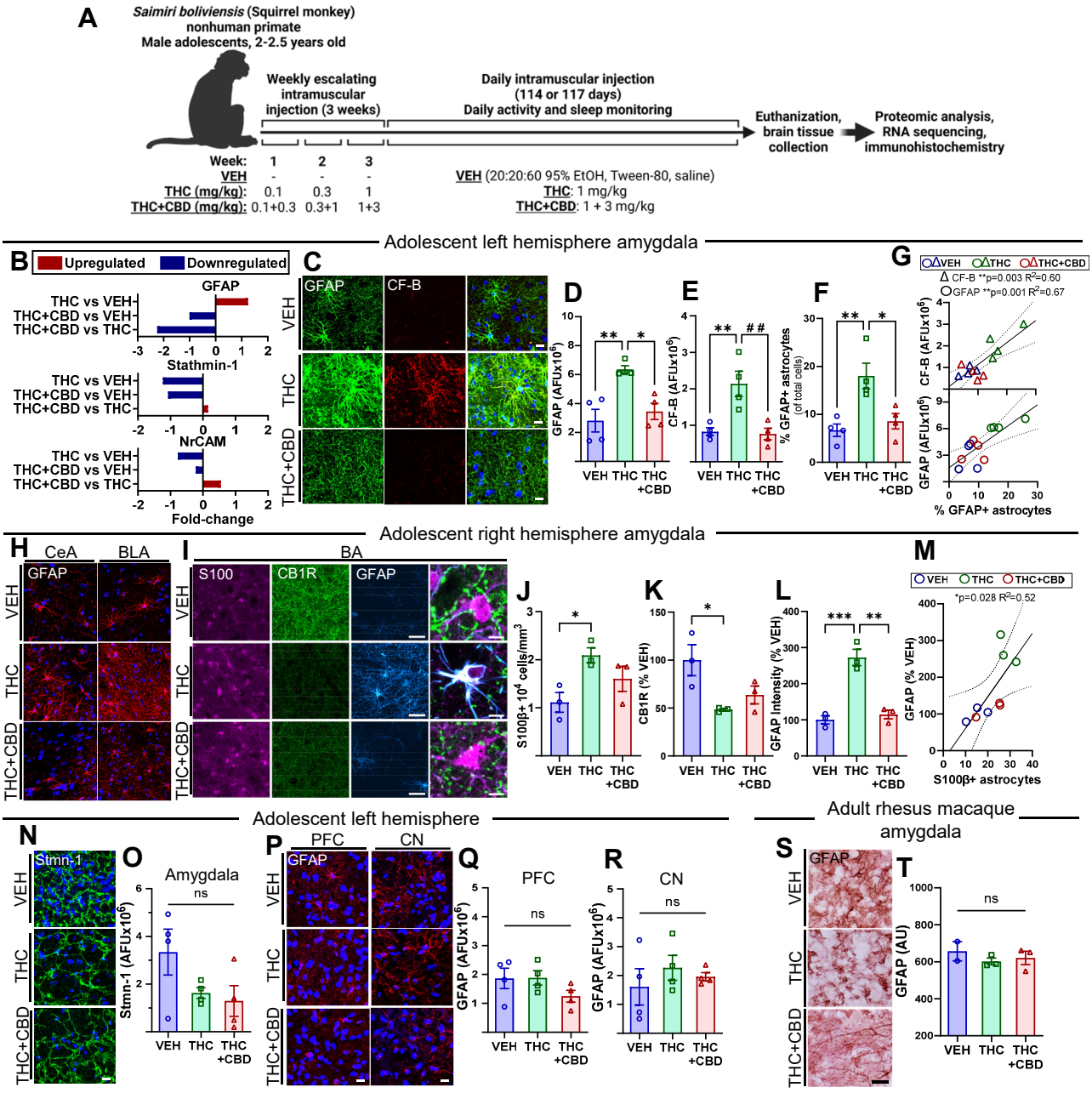

Figure 1. Exposure to THC in adolescence induces proinflammatory astrogliosis in the primate amygdala. **(A)** Drug administration regimen in male adolescent *Saimiri boliviensis* (squirrel monkey) primates. **(B)** Proteomic analysis of differentially expressed proteins in adolescent primate amygdala (n = 3 per group) for GFAP (THC vs. VEH q = .7884, THC+CBD vs. VEH q = 1.000, THC+CBD vs. THC q = .0463), stathmin-1 (THC vs. VEH $q = 2.487 \times 10^{-5}$, THC+CBD vs. VEH q = .0446, THC+CBD vs. THC q = .0197), and NrCAM (THC vs. VEH q = .0093, THC+CBD vs. VEH q = 1.000, THC+CBD vs. THC q = .0197). **(C)** GFAP and CF-B IHC from adolescent primate left hemisphere amygdala, scale bar = 10 μm. **(D, E)** GFAP and CF-B fluorescence (AFU), n = 4 per group (GFAP: p = .004, $F_{2,9}$ = 10.83, post hoc: $^{**}p$ = .0046, $^{*}p$ = .0147. CF-B: p = .0031, $F_{2,9}$ = 11.73, post hoc: $^{**}p$ = .0069, $^{\#\#}p$ = .0051). **(F)** GFAP+ fraction of total cell density, n = 4 (p = .0057, $F_{2,9}$ = 9.696; post hoc: $^{**}p$ = .0067, $^{*}p$ = .0187). **(G)** Pearson's 2-tailed correlation, linear regression and 95% CI between percentage (%) GFAP-positive astrocytes and CF-B (top), GFAP (bottom), p and R^2 values above plots. **(H)** GFAP IHC from adolescent primate right hemisphere CeA and BLA, scale bar = 10 μm. **(I)** S100β, CB1R, GFAP IHC from adolescent primate right hemisphere BA (n = 3 per group). Scale bars = 40 μm for nonmagnified images, 5 μm for magnified images (last column). **(J)** Amygdala S100β-positive cells/mm^3 (p = .0471, $F_{2,6}$ = 5.308; post hoc: $^{*}p$ = .0396). **(K, L)** Amygdala CB1R and GFAP fluorescence intensity as % of vehicle (CB1R: p = .0371, $F_{2,6}$ = 5.998, post hoc: $^{*}p$ = .0346. GFAP: p = .0005, $F_{2,6}$ = 35.58, post hoc: $^{***}p$ = .0007, $^{**}p$ = .0011). **(M)** Pearson's 2-tailed correlation, linear regression, and 95% CI between S100β-positive astrocytes and GFAP, p and R^2 value above plot. **(N, O)** Stathmin-1 IHC and quantification from adolescent primate left hemisphere amygdala, n = 4 (p = .1269, $F_{2,9}$ = 2.619). **(P–R)** GFAP IHC and quantification from adolescent PFC and CN, n = 4 (PFC: p = .5976, $F_{2,9}$ = 0.5455; CN: p = .2337, $F_{2,9}$ = 1.716). Scale bar = 10 μm. **(S, T)** GFAP IHC with quantification from adult Rhesus macaque primate amygdala, n = 2–3 per group (p = .5879, $F_{2,9}$ = 0.5919). Scale bar = 50 μm. All bar graphs show mean ± SEM and were analyzed by 1-

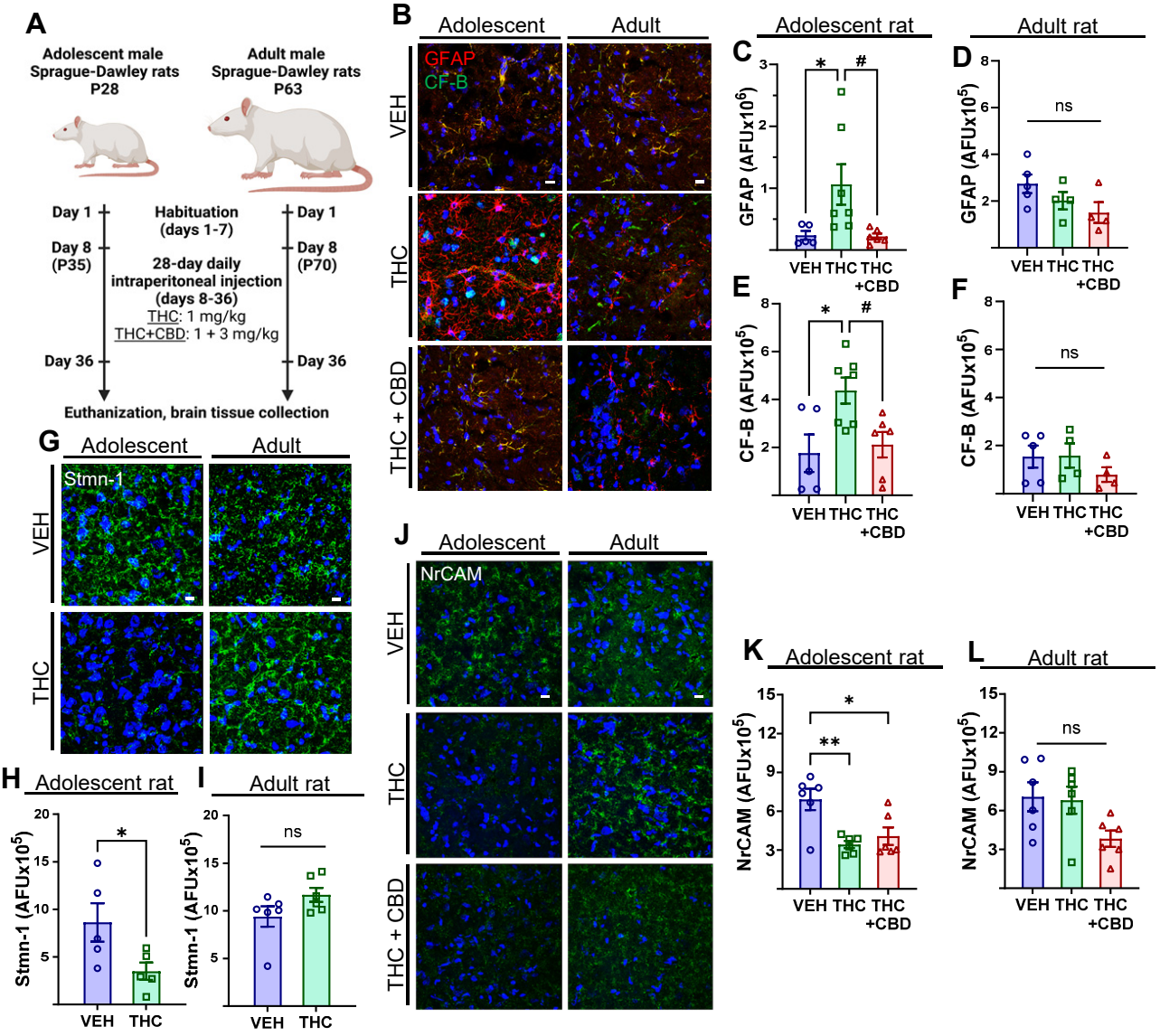

Figure 2. Adolescent but not adult exposure to THC induces proinflammatory astrogliosis with reduced stathmin-1 and NrCAM expression in rat amygdala. **(A)** Schematic of chronic drug administration regimen in male adolescent (P35) and adult (P70) Sprague-Dawley rats. **(B)** Rat amygdala GFAP and CF-B fluorescent IHC from vehicle (adolescent n = 5, adult n = 5), THC (adolescent n = 7, adult n = 4), and THC+CBD (adolescent n = 5, adult n = 5), scale bar = 15 μm. **(C–F)** Amygdala GFAP fluorescence values (AFUs) for adolescent rat (GFAP: Brown–Forsythe ANOVA, p = .0306, $W_{2.000,8.715}$ = 3.013; Welch's post hoc test: $^{*}p$ = .0456, $^{\#}p$ = .0422. CF-B: p = .0141, $F_{2,15}$ = 5.744; post hoc: $^{*}p$ = .0229, $^{\#}p$ = .0387) and adult rat (GFAP: p = .1400, $F_{2,10}$ = 2.408; CF-B: p = .4036, $F_{2,10}$ = 0.9950). **(G)** Amygdala stathmin-1 IHC from vehicle- (adolescent n = 5, adult n = 6) and THC (adolescent n = 5, adult n = 6)-treated rats, scale bar = 15 μm. **(H, I)** Amygdala stathmin-1 fluorescence values for adolescent rat (2-tailed unpaired parametric t test, $^{*}p$ = .0498, t_8 = 2.309) and adult rat (2-tailed unpaired parametric t test, p = .1123, t_{10} = 1.741). **(J)** Amygdala NrCAM IHC from vehicle-, THC-, and THC+CBD-treated rats (n = 6 per age and treatment), scale bar = 15 μm. **(K,L)** Amygdala NrCAM levels (AFU) for adolescent rats **(K)** (p = .0035, $F_{2,15}$ = 8.464; post hoc: $^{**}p$ = .0041, $^{*}p$ = .0171) and adult rats **(L)** (p = .0549, $F_{2,15}$ = 3.543). All bar graphs show mean ± SEM and significance derived from post hoc analysis. Unless otherwise indicated, data were analyzed by 1-way ANOVA with Tukey's post hoc tests. AFU, arbitrary fluorescent unit; ANOVA, analysis of variance; CBD, cannabidiol; CF-B, complement factor-B; GFAP, glial fibrillary acid protein; IHC, immunohistochemistry; P, postnatal day; THC, Δ^9-tetrahydrocannabinol; NrCAM, neuronal cell adhesion molecule; ns, nonsignificant; VEH, vehicle.

way analysis of variance with Tukey's post hoc tests. All significance symbols displayed in graphs for comparisons are derived from post hoc analysis. AFU, arbitrary fluorescence units; AU, arbitrary units; BA, basal amygdala; BLA, basolateral amygdala; CB1R, CB_1 receptor; CBD, cannabidiol; CeA, central amygdala; CN, caudate nucleus; CF-B, complement factor-B; GFAP, glial fibrillary acid protein; IHC, immunohistochemistry; NrCAM, neuronal cell adhesion molecule; ns, nonsignificant; PFC, prefrontal cortex; THC, Δ^9-tetrahydrocannabinol; VEH, vehicle.

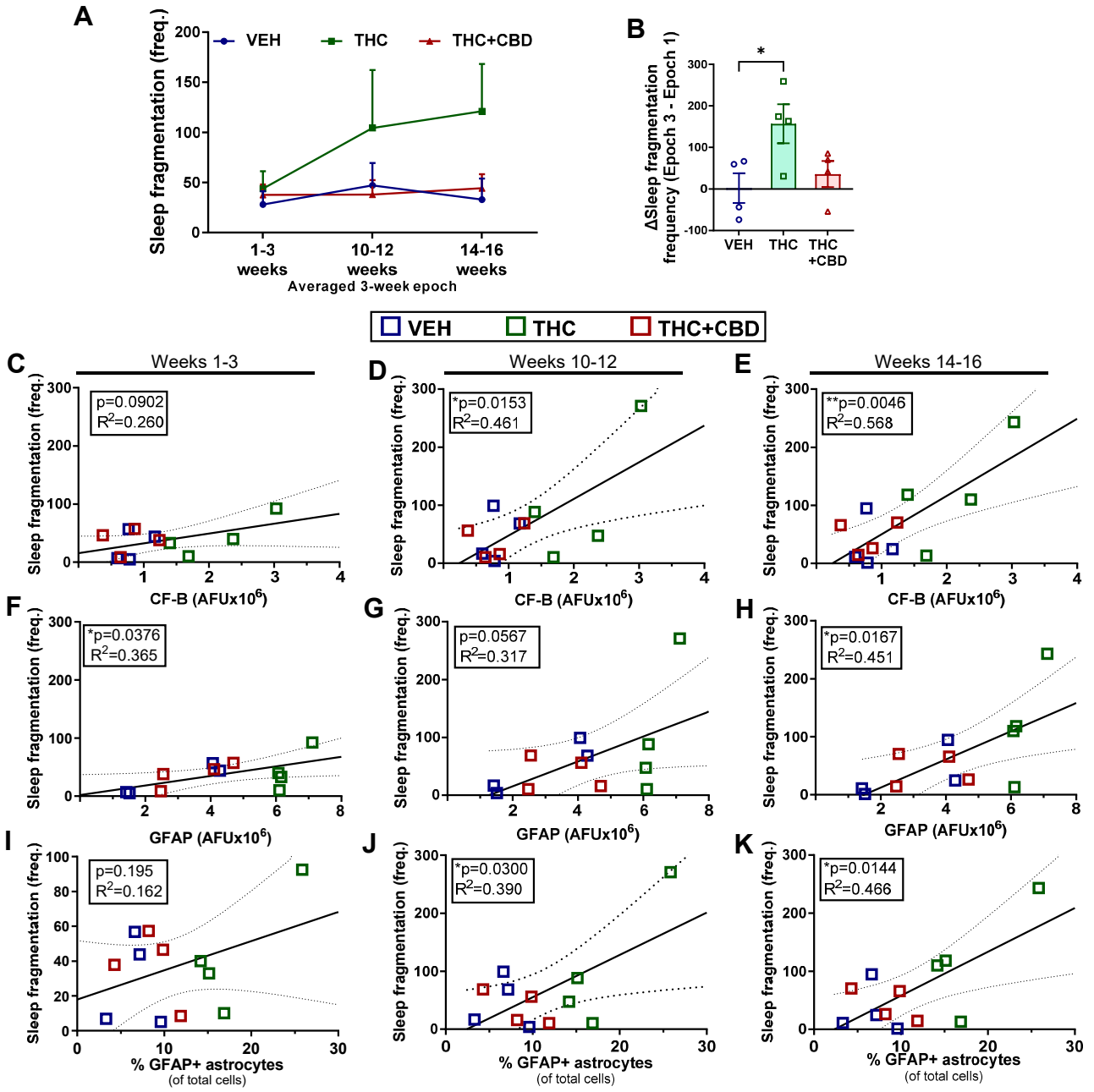

Figure 3. THC-induced sleep disruption is correlated with astrogliosis levels in nonhuman primate amygdala. **(A)** Trajectory of adolescent primate sleep fragmentation frequency over time represented as mean of 3-week epochs for vehicle (n = 4), THC (n = 4), and THC+CBD (n = 4). **(B)** Individual values with mean ± SEM for difference in sleep fragmentation frequency between averaged last 3 weeks of drug administration and first 3 weeks of drug administration in treated adolescent primates (1-way analysis of variance, p = .0457, $F_{2,9}$ = 4.432; Tukey's post hoc test, *p = .0471). **(C–K)** Pearson's 2-tailed correlation analysis between sleep fragmentation frequency detected during weeks 1 to 3, 10 to 12, and 14 to 16 of drug administration with amygdala CF-B **(C–E),** GFAP **(F–H)**, and proportion of GFAP-positive cells **(I–K)** for vehicle-, THC-, and THC+CBD-treated adolescent primate (n = 4 per group). CF-B and GFAP expression levels are expressed as AFUs, quantified from treated adolescent primate amygdala immunohistochemistry. Pearson's 2-tailed analysis with linear regression was performed for all correlation data; 95% CI, p, and R^2 values are indicated within all graphs. Individual subjects are plotted for all correlations. AFU, arbitrary fluorescence unit; CBD, cannabidiol; CF-B, complement factor-B; GFAP, glial fibrillary acid protein; NrCAM, neuronal cell adhesion molecule; THC, Δ^9-tetrahydrocannabinol; VEH, vehicle.

correlated (Figure 3C, F, I). During weeks 10 to 12, CF-B expression and astrocyte numbers were positively correlated with sleep fragmentation frequency (Figure 3D, J). By the final 3 weeks of drug administration, the expressions of CF-B, GFAP, and astrocyte numbers were all positively and significantly correlated with sleep fragmentation frequency (Figure 3E, H, K).

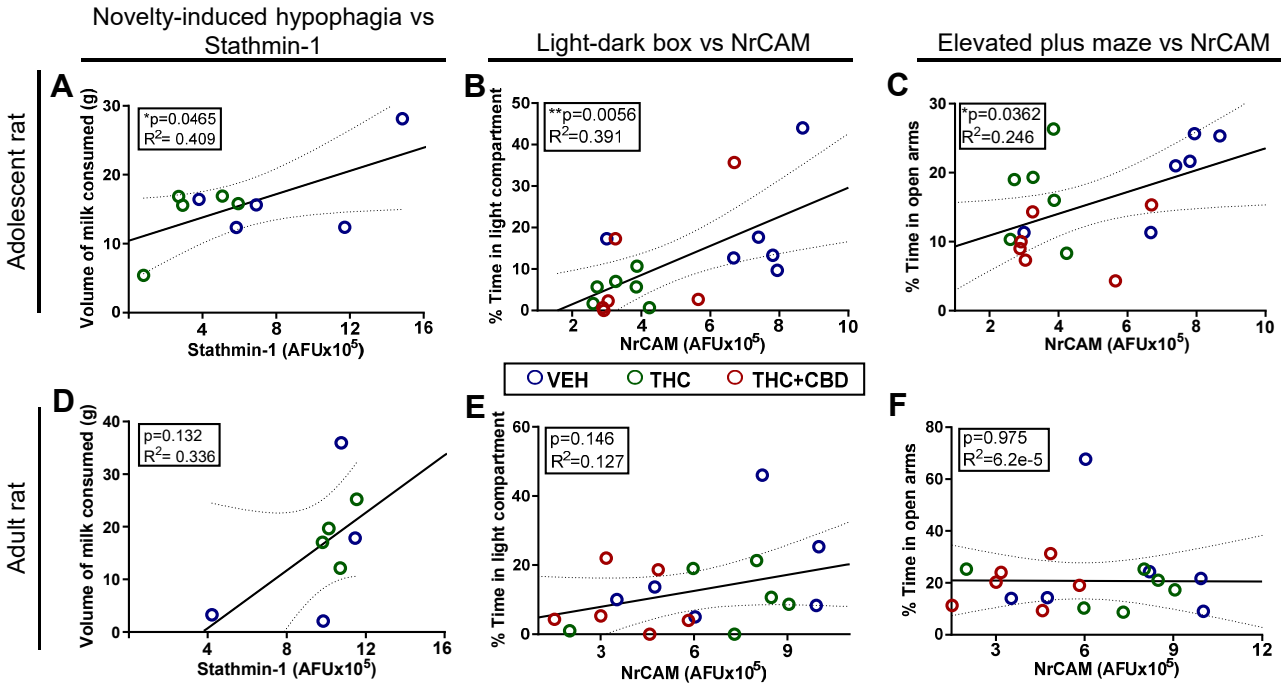

Figure 4. Attenuation of amygdala stathmin-1 and NrCAM expression by THC and THC+CBD are correlated with anxiety-like behaviors in adolescent but not adult rats. Correlation between the volume of milk consumed during the novelty-induced hypophagia test and amygdala stathmin-1 levels (AFU) in adolescent **(A)** and adult **(D)** vehicle-treated (adolescent $n = 5$, adult $n = 4$) and THC-treated (adolescent $n = 5$, adult $n = 4$) rats. Correlation between light-dark box percentage time in light compartment **(B, E)** or elevated plus maze percentage time in open arms **(C, F)** with amygdala NrCAM levels (AFU) for rats treated with vehicle (adolescent $n = 6$, adult $n = 6$), THC (adolescent $n = 6$, adult $n = 6$), and THC+CBD (adolescent $n = 5$, adult $n = 5$). Pearson's 2-tailed correlation analysis with linear regression was performed for all data; 95% CI, p, and R^2 values are indicated within all graphs. Individual subjects are plotted for all correlations. AFU, arbitrary fluorescence unit, CBD, cannabidiol; NrCAM, neuronal cell adhesion molecule; THC, Δ^9-tetrahydrocannabinol; VEH, vehicle.

Stathmin-1 levels were not correlated with sleep disturbance measures at any sampling epoch (Figure S3).

Levels of GFAP or CF-B in amygdala of adolescent rats exposed to THC were not correlated with anxiety and emotionality (Figure S4B–E) (40). However, amygdala stathmin-1 levels in adolescent but not adult rats were significantly and positively correlated with milk consumption volume during the novelty-induced hypophagia test (Figure 4A, D) (40). Amygdala NrCAM in adolescent rats was significantly and positively correlated with anxiety-like behavioral measures of reduced light-dark box light compartment time and reduced elevated plus maze open arm time (Figure 4B, C), with a lack of correlation for adults (Figure 4E, F). These results suggest that chronic adolescent THC exposure conferring glial reactivity may be selectively implicated in disordered sleep, whereas reduction in plasticity-regulating stathmin-1 and NrCAM are implicated in anxiety-related behaviors.

Role of the CB1R in THC-Induced Inflammatory Response in Astrocytes

To investigate whether the THC-induced inflammatory response observed in vivo is mediated by direct astrocyte activation, THC effects were investigated in a primary astrocyte culture model using brains from P1 to P2 rat pups as a source of astrocytes (Figure 5A). CB1R protein and messenger RNA (*Cnr1*) were detected in cultured astrocytes (Figure 5B). Quantification of *Gfap*-positive cells confirmed astrocyte enrichment (>95% *Gfap*+), with ~40% of *Gfap*+ astrocytes in culture expressing *Cnr1* (Figure 5C).

To model the drug administration paradigm carried out in vivo, primary astrocyte cultures were treated with daily THC or THC+CBD over 72 hours followed by assessment of reactive astrocyte markers. Repeated THC exposure increased expression of GFAP, CF-B, S100β, and complement C3, and CBD co-treatment reduced reactive marker upregulation (Figure 5E–H). Transition to astrocyte reactivity was accompanied by morphological changes, including astrocyte hypertrophy (24); therefore, astrocyte size was evaluated. Repeated THC increased astrocyte cell size and induced multinucleation, indicating reactive hypertrophy (41), and co-treatment with CBD decreased THC-induced hypertrophy (Figure 5I, J and Figure S6A).

To investigate whether CB1R activation mediated these effects, THC was introduced to astrocytes following pre-incubation with the CB1R inverse agonist rimonabant. Rimonabant decreased THC-induced rises in GFAP, CF-B, S100β, and C3 (Figure 5K–O). CB1R blockade with rimonabant pre-treatment also reduced THC-induced astrocyte hypertrophy (Figure 5P, Q), suggesting that THC via CB1R activation acts directly on astrocytes to result in gliosis that is reversed by CBD.

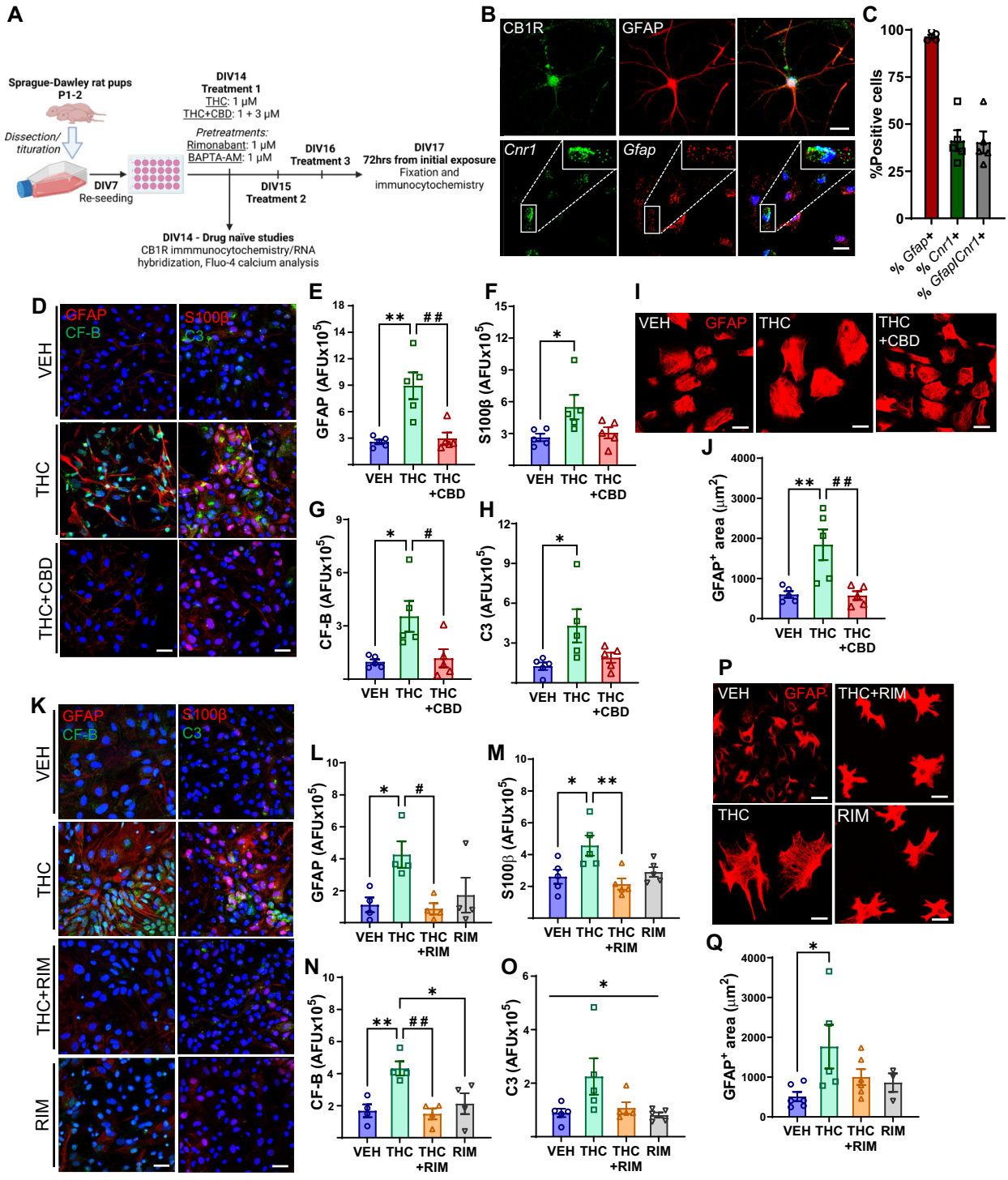

Figure 5. THC induces CB1R-dependent transition to reactive astrocyte phenotype in primary astrocyte cultures. **(A)** Experimental design for in vitro primary astrocyte culture experiments. **(B)** GFAP-positive primary rat astrocytes showing CB1R protein (top, CB1R) and mRNA (bottom, *Cnr1*) levels, scale bars = 10 μm. **(C)** In situ mRNA % positivity quantification for *Gfap*, *Cnr1*, and *Gfap*/*Cnr1* in primary astrocyte cultures ($n = 5$). **(D)** GFAP, CF-B, S100β, complement C3 primary astrocyte ICC following daily treatment for 72 hours with vehicle, 1 μM THC, and 1 μM THC + 3 μM CBD. **(E–H)** Primary astrocyte GFAP, S100β, CF-B, and C3 fluorescence values (AFU) following THC and THC+CBD treatment [$n = 5$. **(E)** GFAP: $p = .0009$, $F_{2,12} = 13.42$. Post hoc: $^{**}p = .0016$, $^{\#\#}p = .0026$. **(F)** S100β: $p = .0425$, $F_{2,12} = 4.157$. Post hoc: $^{*}p = .0492$. **(G)** CF-B: $p = .0165$, $F_{2,12} = 5.889$. Post hoc: $^{*}p = .0236$, $^{\#}p = .0369$. **(H)** C3: $p = .0391$, $F_{2,12} = 4.301$. Post hoc: $^{*}p = .0408$]. **(I, J)** GFAP-positive primary astrocytes treated daily for 72 hours with vehicle, THC, and THC+CBD as above, used for surface area quantification [$n = 5$. **(J)** $p = .0035$, $F_{2,12} = 9.424$. Post hoc: $^{**}p = .0077$, $^{\#\#}p = .0066$]. **(K)** GFAP, CF-B, S100β, C3 primary astrocyte ICC following daily treatment

Roles of Intracellular Calcium Signaling in THC-Induced Reactive Astrogliosis

Because calcium signaling cascades are a main conduit by which astrocytes execute inflammatory functions, THC effects on CB1R-mediated calcium signaling were investigated. THC acutely and rapidly increased intracellular calcium release in cultured astrocytes (Figure 6A), which was blocked by rimonabant, indicating CB1R-specific activation of calcium signaling (Figure 6A, B). To investigate specific calcium signaling cascades downstream of CB1R activation by THC, the IP_3 receptor (IP3R) inhibitor 2-APB was used, which attenuated calcium signaling by THC activation (Figure 6C, D). Since CB1R activation by THC elicits IP3R-dependent intracellular calcium signaling, effects of the selective intracellular calcium chelator BAPTA-AM in blocking THC-induced astrocyte reactivity were evaluated. BAPTA-AM pretreatment blocked THC-induced elevations of GFAP, CF-B, and C3 but did not have a significant effect on S100β (Figure 6E–I). Because GPCR (G protein–coupled receptor)-mediated calcium signaling can be triggered through $G\alpha_q$ activation, the possibility that THC-activated calcium signaling via this mechanism was explored. The inhibitor of $G\alpha_q$ YM-254890 (YM) did not attenuate the THC-induced calcium signal (Figure 6J, K). In summary, repeated THC exposure induced astrocyte reactivity through a CB1R-activated IP3R calcium signaling cascade.

Age-Dependent Sensitivity to THC and CB1R Expression in Neurons and Astrocytes

Immunohistochemical and in situ hybridization results in adolescent primate amygdala and primary cultured rat astrocytes showed robust expression of astrocytic CB1R (Figures 1I and 5B). Therefore, the potential contribution of astrocyte CB1R developmental differences to mediating vulnerability to THC-induced astrogliosis was explored. Qualitative analysis of adolescent nonhuman primate amygdala showed CB1R colocalization within GFAP-positive astrocytes, with lower levels in NeuN-positive neurons, indicating astrocyte-specific enrichment of CB1R (Figure 7A). In situ hybridization of *Cnr1* mRNA in P35 rat prelimbic cortex (PL), dorsal striatum (DS), nucleus accumbens (NAc) core, and amygdala showed higher proportion of *Cnr1*-positive cells compared with P70 for the same regions (Figure 7B, C). To determine whether astrocyte- or neuron-specific expression of *Cnr1* drives developmental differences in CB1R expression, colocalization of *Cnr1* mRNA with *Gfap* or neuron-specific *Rbfox3* mRNA was assessed. There were no age-related differences in total number of astrocytes and neurons for all regions analyzed (Figure 7D, E). In PL, DS, and the NAc core, there was no difference in *Cnr1*-positive astrocytes at P35 compared with P70 (Figure 7F). However, the density of *Cnr1*-positive neurons was greater at P35 than at P70 (Figure 7G). In stark contrast, the P35 amygdala harbored a greater density of *Cnr1*-expressing astrocytes compared with P70 amygdala, with no differences in density of *Cnr1*-expressing neurons between the 2 ages (Figure 7F, G). These results suggest that the age-related differences in amygdala *Cnr1* levels are largely driven by augmented expression in astrocyte cellular fractions, whereas those in cortical and striatal brain regions are conferred primarily by neuronal expression. Thus, the basally elevated astrocyte-specific expression of CB1R in the adolescent amygdala may drive the heightened sensitivity of astrocytes to THC, whereas the absence of developmental differences in astrocytic CB1R in the adolescent cortex and striatum may spare these regions from the inflammatory, glial-activating effects of THC.

DISCUSSION

Initiation of daily cannabis use at early ages can trigger neurodevelopmental modifications, potentially increasing adolescent and lifetime susceptibility to psychiatric symptoms and disorders. In this study examining the impact of THC on adolescent nonhuman primate and rat, our central focus was the amygdala, wherein proteomic analysis provided leads that revealed marked induction of proinflammatory astrocyte reactivity and decreased neurodevelopmental proteins stathmin-1 and NrCAM. Co-administration of CBD blocked the proinflammatory effects of THC. In stark divergence from adolescents, amygdala of adult rat following THC treatment did not have comparable changes. Astrocyte reactivity measures in adolescent nonhuman primate were positively correlated with sleep fragmentation, and stathmin-1 and NrCAM levels were correlated with increased anhedonic- and anxiety-like behavior in adolescent rat. Primary astrocyte cultures revealed direct activation of astrocyte CB1R- and IP3R-mediated intracellular calcium signaling by THC, triggering proinflammatory activation, an effect also attenuated by CBD. Finally, elevated expression of astrocyte CB1R within the adolescent amygdala likely contributed to heightened vulnerability to cannabis during this critical period of maturation.

Astrocytes may react to injury or neurological disease process with reactive astrogliosis responses, characterized by upregulation of GFAP, S100β, and C3 hypertrophy and an increase in numbers (42,43), which may trigger repair processes but may also prolong or exacerbate a neurological disease state (37). The upregulated GFAP in amygdala of THC-treated adolescent primate and rat was paralleled by decreased amygdala *Gfap* gene transcript in an RNA sequencing analysis from the same primate cohort. A mismatch of astrocyte protein and transcript level has been reported in adult rat amygdala

for 72 hours with vehicle, THC, THC+RIM, and RIM at a dose of 1 μM for each drug. **(L–O)** Primary astrocyte GFAP, S100β, CF-B, and C3 fluorescence values following THC, THC+RIM, and RIM treatment [n = 4–5. **(L)** GFAP: p = .0272, $F_{3,12}$ = 4.349. Post hoc: $^{*}p$ = .0487, $^{\#}p$ = .0324. **(M)** S100β: p = .0085, $F_{3,16}$ = 5.521. Post hoc: $^{*}p$ = .0325, $^{**}p$ = .0074. **(N)** CF-B: p = .0040, $F_{3,12}$ = 7.665. Post hoc: $^{**}p$ = .0089, $^{\#\#}p$ = .0054, $^{*}p$ = .0282. **(O)** C3: p = .0471, $F_{3,16}$ = 3.308]. **(P, Q)** GFAP-positive primary astrocytes treated daily for 72 hours with vehicle, THC, THC+RIM, and RIM as above, for surface area quantification [**(Q)** n = 3–6, p = .0644, $F_{3,16}$ = 2.948; post hoc: $^{*}p$ = .0435]. All data were analyzed by 1-way analysis of variance with Tukey's post hoc analysis and presented as mean ± SEM, scale bar = 30 μm unless otherwise indicated. AFU, arbitrary fluorescence unit; CB1R, CB_1 receptor; CBD, cannabidiol; CF-B, complement factor-B; DIV, days in vitro; GFAP, glial fibrillary acid protein; ICC, immunocytochemistry; mRNA, messenger RNA; RIM, rimonabant; THC, Δ^9-tetrahydrocannabinol; VEH, vehicle.

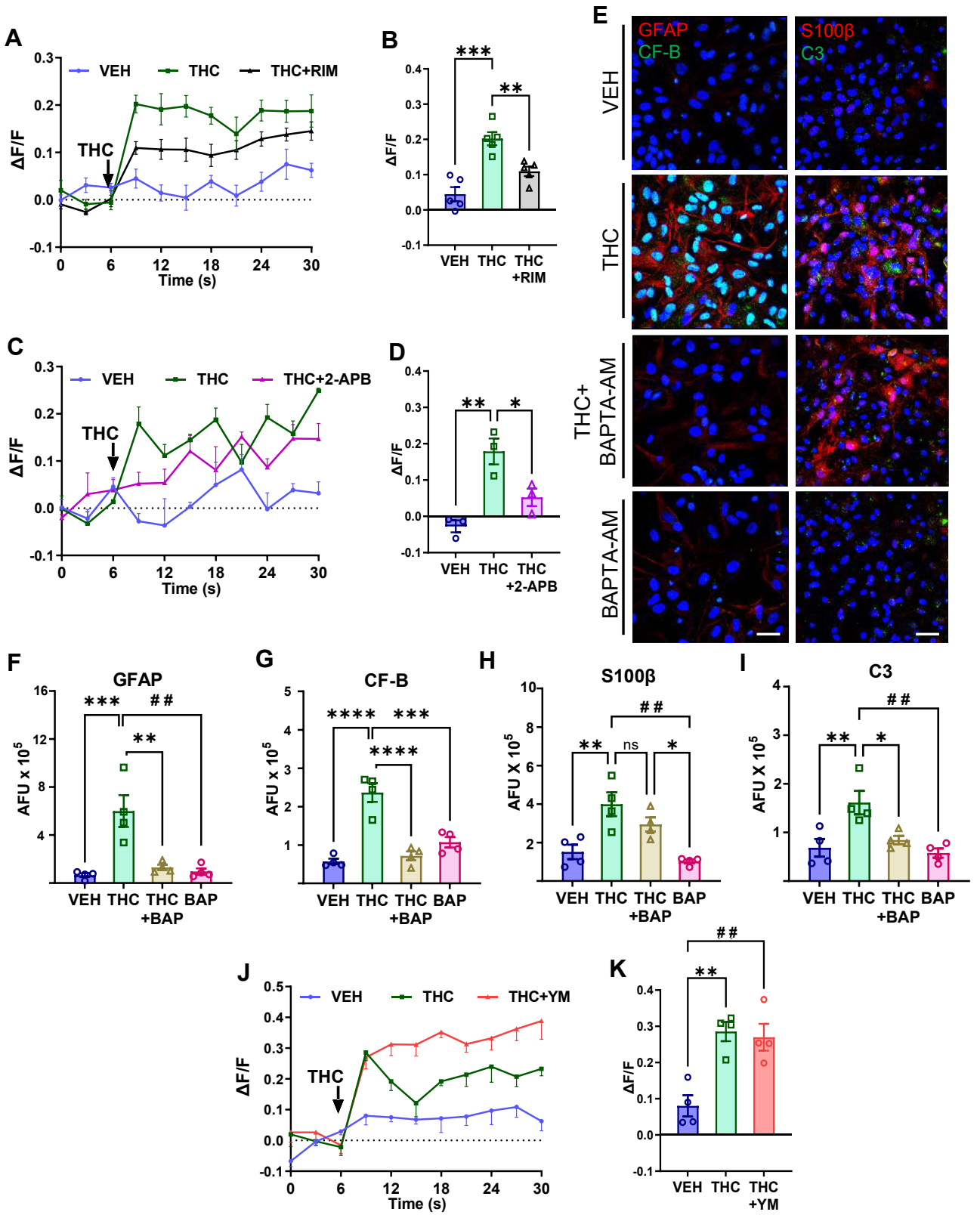
A
VEH
THC
THC+RIM
THC
ΔF/F
Time (s)
B
***
**
ΔF/F
VEH THC THC +RIM
C
VEH
THC
THC+2-APB
THC
ΔF/F
Time (s)
D
**
*
ΔF/F
VEH THC THC +2-APB
E
GFAP
CF-B
S100β
C3
VEH
THC
THC+ BAPTA-AM
BAPTA-AM
F
GFAP
AFU x 10^5
VEH THC THC +BAP BAP
G
CF-B
AFU x 10^5
VEH THC THC +BAP BAP
H
S100β
AFU X 10^5
ns
VEH THC THC +BAP BAP
I
C3
AFU X 10^5
VEH THC THC +BAP BAP
J
VEH
THC
THC+YM
THC
ΔF/F
Time (s)
K
ΔF/F
VEH THC THC +YM

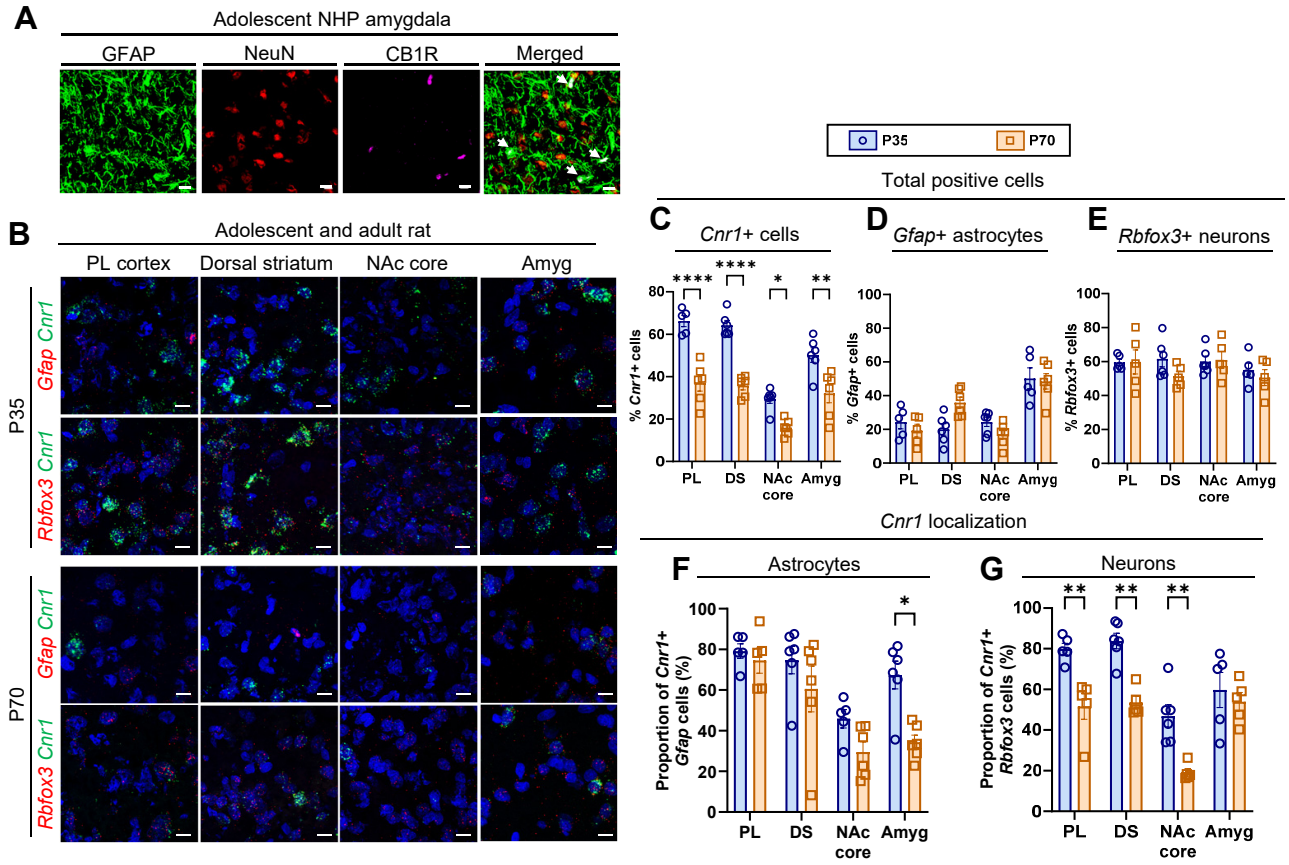

Figure 7. Developmentally regulated CB1R expression in neurons and astrocytes. **(A)** Immunohistochemistry images from adolescent nonhuman primate amygdala showing colocalization of CB1R with GFAP-labeled cells and lower colocalization levels with NeuN-positive cells. White arrows indicate sites of CB1R-GFAP colocalization. **(B)** Representative in situ messenger RNA hybridization images of *Cnr1* with *Gfap* and *Rbfox3* in adolescent (P35, n = 5–6) and adult (P70, n = 5–6) rat PL, DS, NAc core, and amygdala. **(C)** Quantified percentage of total *Cnr1*-positive cells on P35 compared with P70 (brain region $F_{3,39}$ = 40.42, ****$p < .0001$; age $F_{1,39}$ = 114.5, ****$p < .0001$; brain region × age interaction $F_{3,39}$ = 3.46, *$p = .025$), for PL (****$p < .0001$), DS (****$p < .0001$), NAc core (*$p < .042$), and amygdala (**$p = .0019$). **(D)** Percentage of total *Gfap*-positive cells in P35 and P70 rat brain (brain region $F_{3,37}$ = 22.87, ****$p < .0001$; age $F_{1,37}$ = 0.026, $p = .87$; brain region × age interaction $F_{3,37}$ = 3.84, *$p = .017$). **(E)** Percentage of total *Rbfox3*-positive cells in P35 and P70 rat brain (brain region $F_{3,34}$ = 1.24, $p = .31$; age $F_{1,34}$ = 1.15, $p = .29$; brain region × age interaction $F_{3,34}$ = 0.70, $p = .56$). **(F)** Proportion of *Cnr1*-positive *Gfap*-expressing astrocytes in P35 or P70 rat brain (brain region $F_{3,37}$ = 13.2, ****$p < .0001$; age $F_{1,37}$ = 13.12, ***$p = .0009$; brain region × age interaction $F_{3,37}$ = 1.6, $p = .21$; P35 vs. P70 amygdala *$p = .17$). **(G)** Proportion of *Cnr1*-positive *Rbfox3*-expressing neurons in P35 or P70 rat brain (brain region $F_{3,34}$ = 21.4, ****$p < .0001$; age $F_{1,34}$ = 41.9, ****$p < .0001$; brain region × age interaction $F_{3,34}$ = 2.6, $p = .071$; P35 vs. P70 PL **$p = .0094$, DS **$p = .0027$, NAc core **$p = .0071$, amygdala $p = .99$). All scale bars = 10 μm, data were analyzed by 2-way analysis of variance with Tukey's post hoc tests, presented as mean ± SEM. Amyg, amygdala; CB1R, cannabinoid type-1 receptor; DS, dorsal striatum; GFAP, glial fibrillary acid protein; NAc, nucleus accumbens; NHP, nonhuman primate; P, postnatal day; PL, prelimbic cortex.

Figure 6. THC activates CB1R to elicit intracellular calcium signaling via IP_3 receptors in astrocytes to induce astrogliosis. **(A, C)** Intracellular calcium levels detected by Fluo-4 in primary rat astrocytes across 11 reads over 30 seconds with acute stimulation by vehicle or THC with rimonabant **(A)** (n = 5) or **(C)** 2-APB (n = 3) pretreatment. Arrow indicates addition of THC. Data are mean + SEM. **(B, D)** Calcium levels immediately after acute vehicle or THC with RIM **(B)** (p = .0001, $F_{2,12}$ = 20.20; post hoc: ***p = .0001, **p = .0075) or 2-APB **(D)** (p = .0044, $F_{2,6}$ = 15.37; post hoc: **p = .0037, *p = .0345). Data are mean ± SEM. **(E)** GFAP, CF-B, S100β, and complement C3 primary astrocyte immunocytochemistry following 72 hours treatment with vehicle, 1 μM THC, 1 μM THC + 10 μM BAPTA-AM, and 10 μM BAPTA-AM. Scale bar = 10 μm. **(F–I)** Primary astrocyte GFAP, CF-B, S100β, and C3 fluorescence values following THC and BAPTA-AM treatments, n = 4 [**(F)** GFAP: p = .0004, $F_{3,12}$ = 13.48; post hoc: ***p = .0007, **p = .0020, ##p = .0011. **(G)** CF-B: $p < .0001$, $F_{3,12}$ = 27.61; post hoc: ****$p < .0001$, ***p = .0004. **(H)** S100β: p = .0009, $F_{3,12}$ = 10.99; post hoc: **p = .0051, ##p = .0012, *p = .0269. **(I)** C3: p = .0032, $F_{3,12}$ = 8.123; post hoc: **p = .0083, *p = .0280, ##p = .0038]. **(J)** Fluo-4 measurement of intracellular calcium in primary rat astrocytes across 11 reads over 30 seconds with acute stimulation by vehicle or THC with YM (n = 4). Data are mean + SEM. **(K)** Calcium levels immediately after addition of vehicle or THC with YM (p = .0020, $F_{2,9}$ = 13.35; post hoc: **p = .0031, ##p = .0052). Data are mean ± SEM. All data were analyzed by 1-way analysis of variance with Tukey's post hoc analysis. Significance symbols displayed for comparisons are derived from post hoc statistical tests. 2-APB, 2-aminoethoxydiphenylborate; AFU, arbitrary fluorescence unit; CB1R, CB_1 receptor; CF-B, complement factor-B; GFAP, glial fibrillary acid protein; RIM, rimonabant; THC, Δ^9-tetrahydrocannabinol; VEH, vehicle; YM, YM-254890.

following adolescent stress and high-dose THC (5 mg/kg) exposure, resulting in increased BLA astrocyte:neuron ratios but decreased astrocyte-specific gene transcripts (44). Thus, evaluating RNA species in isolation may not accurately reflect functional protein levels, particularly in analyses with active neuroinflammation, which recruit mechanisms that suppress RNA translational machinery (45).

The effects of THC on GFAP expression exhibit a nuanced relationship depending on brain region, dosage, sex, astrocyte heterogeneity, age of exposure, and time postexposure (46–48). Notably here, the inflammatory astrocyte reaction induced by THC exclusively in adolescent amygdala stands out, as GFAP was unaffected in the striatum and PFC. GFAP was unchanged in adult rhesus monkeys treated with THC, although there are limitations posed by the fact that the primate species differed from the adolescent squirrel monkeys used in the main study. Nonetheless, the results obtained in the available adult primate species indicated the possibility of an intriguing age-related divergence in THC-induced amygdala astrogliosis, leading to the undertaking of species-, age-, and treatment duration-controlled investigations in rat, which confirmed the distinctive adolescent amygdala-specific vulnerability to THC-induced astrogliosis.

Increased GFAP following adolescent THC exposure indicated an inflammatory, reactive astrocyte phenotype in the amygdala, which was confirmed by astrocyte CF-B and C3 upregulation. Controlled inflammatory activity is critical for neurodevelopmental synaptic pruning (49,50). However, inflammatory complement factors are also implicated in the etiology of psychiatric disorders associated with adolescent cannabis exposure if inappropriately activated. Aberrant complement function has been linked to schizophrenia (51,52), depression (53), and anxiety (54), suggesting an overlapping contribution of this inflammatory pathway in cannabis-associated psychiatric pathology. THC-induced CF-B and C3 upregulation may drive aberrant pruning in the amygdala to the detriment of establishing appropriate neural connectivity yet to develop during adolescence, thereby dysregulating its behavioral outputs to predispose users to psychiatric disorders. Consistent with this, a correlation was found between the established early psychiatric disturbance marker of sleep fragmentation (55) and astrocyte reactivity measures. Despite the limited subject pool and notable variability, correlations between certain reactivity markers were apparent even at weeks 1 to 3 of THC exposure, suggesting that astrocyte-linked sleep disruption is detectable early in the course of THC exposure during adolescence, whereas CBD co-administration reversed both astrocyte reactivity and sleep disruption.

Amygdala astrocyte reactivity may underlie the higher prevalence of sleep disturbance observed in adolescent chronic cannabis users (56) given the central role of astrocytes in maintaining circadian and sleep-wake functions (57). Reactive astrocytes have been shown to alter cellular homeostasis, promoting sleep fragmentation to decrease sleep quality through altered transmitter release and reuptake normally regulating sleep (58–60). Altered serum or cerebrospinal fluid levels of GFAP and astrocyte-specific gliotransmitter kynurenic acid have been found in patients with sleep disorders and in healthy participants following sleep deprivation, reflecting perturbed astrocyte function in states of disrupted sleep (61,62).

Proteomic and immunohistochemical analysis of the amygdala also revealed an adolescent-specific reduction in stathmin-1, a microtubule destabilizer that exhibits enrichment in the lateral amygdala during juvenile brain development and is involved in innate and learned fear behavior (33,34). Similarly, adolescent amygdala exhibited reduced NrCAM, a neuronal and astrocytic protein with critical roles in GABAergic (gamma-aminobutyric acidergic) synaptic maturation and contextual fear learning (35,36,63,64). We found significant positive correlations between adolescent amygdala stathmin-1 and NrCAM levels and anxiety-like behavioral measures, whereas no correlation between stathmin-1 and sleep was found.

While CBD co-administration mitigated the effects of THC-induced astrocyte reactivity, it had no effect on THC-induced reduction of stathmin-1 and NrCAM levels. These results are consistent with established evidence that CBD counteracts certain but not all behavioral or molecular effects of THC (65,66). In the same adolescent primates, CBD did not mitigate impaired cognition but did prevent THC-induced emesis (39). To elucidate the effects of THC on astrocytes, a primary astrocyte culture model was used to demonstrate the direct activation of CB1R-mediated astrocyte calcium signaling in initiating reactive transformation, with reversal by CBD co-treatment. The anti-inflammatory CBD actions may be mediated by its negative allosteric modulation of astrocyte CB1R to counteract the effects of THC (67). However, CBD has been shown to exhibit neuroprotective effects through astrocyte PPARγ and 5-HT$_{1A}$ receptor activation, among other neuronal and astrocytic targets (68,69). Although it is tempting to speculate about the use of CBD ameliorating negative THC effects, it is important to note that the appropriateness of CBD as a therapeutic agent is still largely undetermined owing to its complex interactions between other (endo)cannabinoids in the developing brain.

Astrocyte calcium signaling has important roles in regulating synaptic transmission and may be triggered by different mechanisms to modulate synaptic transmitter concentrations (70,71). With emerging evidence of endocannabinoid-activated astrocytic calcium pathways in the amygdala (72), it was demonstrated that astrocyte reactivity occurred via CB1R, which was an IP3R-mediated but Gα_q-independent mechanism of calcium mobilization. Consistent with these results, Gα_q-independent mechanisms have been shown in THC-activated astrocytic CB1R via G$\beta\gamma$ (73), although these results may be cellular context- and ligand-dependent (74). Furthermore, G$\beta\gamma$-mediated IP3R activation of intracellular calcium release was found to preferentially occur with Gα_i-coupled receptors (75), such as CB1Rs.

Adolescent rodents harbor elevated CB1R expression in cortical and striatal regions that progressively declines with maturation (11,76), a developmental effect that was shown here to be primarily driven by neuronal CB1R expression. Developmental differences in astrocyte CB1R expression were explored as a contributing factor to age-specific astrogliosis. Although it is known that some astrocytes express CB1R (72,77), we demonstrated robust expression of CB1R in primate and rat amygdala astrocytes and in primary cultured rat astrocytes. In contrast to cortical and striatal regions, the results from rat amygdala astrocytes revealed higher levels of

CB1R in adolescents than in adults, which may drive greater degrees of CB1R-mediated calcium mobilization induced by THC to initiate reactive gliosis. The lack of developmental astrocytic CB1R differences coupled with prominent neuronal CB1R expression in the maturing cortex and striatum may underlie the lack of astrogliosis in these regions following THC exposure in adolescent primate.

Conclusions

Taken together, our results reveal that chronic THC exposure during a critical period of adolescent brain maturation elicited inflammatory activation of astrocytes and attenuated expression of certain proteins in the amygdala, together vital for regulation of sleep and anxiety. These mechanisms underscore the significant detrimental reorganization of the adolescent neuronal and glial landscape within the amygdala following chronic THC exposure, which does not occur in other brain regions or following comparable THC exposure in adult animals. Our results demonstrate a vital mechanism potentially underlying the increased risk of psychiatric disorders involving amygdala dysfunction following chronic cannabis use at a critical developmental stage.

ACKNOWLEDGMENTS AND DISCLOSURES

This work was supported by National Institute on Drug Abuse (Grant No. DA042178 [to BKM and SRG]) and Canadian Institutes of Health Research (Grant No. PJT-148633 [to SRG]).

SRG and BKM conceived the study. SRG, BKM, MS, YS, and MH designed the study experiments. YS, MS, MM, SLW, PG, AG, JB, and M-EDR performed the experiments and collected data. YS, MS, SLW, PG, and AG analyzed and interpreted the data and/or prepared figures. YS, SRG, and BKM wrote the manuscript.

We thank the University of Toronto Donnelly Mass Spectrometry Center personnel Dr. Edyta Marcon and Dr. Shuye Pu for assistance with nonhuman primate proteomic studies. We thank Dr. Ahmed Hasbi for his helpful comments during this study.

The authors report no biomedical financial interests or potential conflicts of interest.

ARTICLE INFORMATION

From the Department of Pharmacology and Toxicology, Temerty Faculty of Medicine, University of Toronto, Toronto, Ontario, Canada (YS, MS, MM, M-EDR, SRG); McLean Hospital, Belmont, Massachusetts (AG, JB, SLW, BKM); Department of Psychiatry, Harvard Medical School, Boston, Massachusetts (AG, JB, SLW, BKM); Picowar Institute for Learning and Memory, Department of Brain and Cognitive Sciences, Massachusetts Institute of Technology, Cambridge, Massachusetts (PG, MH); and Department of Medicine, Temerty Faculty of Medicine, University of Toronto, Toronto, Ontario, Canada (SRG).

YS and MS contributed equally to this work.

Address correspondence to Yalin Sun, Ph.D., at yalin.sun@mail.utoronto.ca, or Susan R. George, M.D., at s.george@utoronto.ca.

Received Sep 9, 2024; revised Feb 24, 2025; accepted Mar 13, 2025.

Supplementary material cited in this article is available online at https://doi.org/10.1016/j.bpsgos.2025.100496.

REFERENCES

1. Zuckermann AME, Gohari MR, Romano I, Leatherdale ST (2021): Changes in cannabis use modes among Canadian youth across recreational cannabis legalization: Data from the COMPASS prospective cohort study. Addict Behav 122:107025.
2. Petrilli K, Ofori S, Hines L, Taylor G, Adams S, Freeman TP (2022): Association of cannabis potency with mental ill health and addiction: A systematic review. Lancet Psychiatry 9:736–750.
3. Zamberletti E, Rubino T (2022): Dos(e)Age: Role of dose and age in the long-term effect of cannabinoids on cognition. Molecules 27:1411.
4. Arseneault L, Cannon M, Poulton R, Murray R, Caspi A, Moffitt TE (2002): Cannabis use in adolescence and risk for adult psychosis: Longitudinal prospective study. BMJ 325:1212–1213.
5. Gobbi G, Atkin T, Zytynski T (2019): Association of cannabis Use in Adolescence and Risk of Depression, Anxiety, and suicidality in Young Adulthood: A Systematic Review and Meta-analysis (vol 76, pg 426, 2019). JAMA Psychiatry 76:447–447.
6. Debenham J, Birrell L, Champion K, Lees B, Yücel M, Newton N (2021): Neuropsychological and neurophysiological predictors and consequences of cannabis and illicit substance use during neurodevelopment: A systematic review of longitudinal studies. Lancet Child Adolesc Health 5:589–604.
7. De Gregorio D, Dean Conway J, Canul ML, Posa L, Bambico FR, Gobbi G (2020): Effects of chronic exposure to low doses of Δ9-tetrahydrocannabinol in adolescence and adulthood on serotonin/norepinephrine neurotransmission and emotional behaviors. Int J Neuropsychopharmacol 23:751–761.
8. Peters KZ, Zlebnik NE, Cheer JF (2022): Cannabis exposure during adolescence: A uniquely sensitive period for neurobiological effects. Int Rev Neurobiol 161:95–120.
9. Arain M, Haque M, Johal L, Mathur P, Nel W, Rais A, *et al.* (2013): Maturation of the adolescent brain. Neuropsychiatr Dis Treat 9:449–461.
10. Gogtay N, Giedd JN, Lusk L, Hayashi KM, Greenstein D, Vaituzis AC, *et al.* (2004): Dynamic mapping of human cortical development during childhood through early adulthood. Proc Natl Acad Sci USA 101:8174–8179.
11. Ellgren M, Artmann A, Tkalych O, Gupta A, Hansen HS, Hansen SH, *et al.* (2008): Dynamic changes of the endogenous cannabinoid and opioid mesocorticolimbic systems during adolescence: THC effects. Eur Neuropsychopharmacol 18:826–834.
12. Meyer HC, Lee FS, Gee DG (2018): The role of the endocannabinoid system and genetic variation in adolescent brain development. Neuropsychopharmacology 43:21–33.
13. Bara A, Ferland JN, Rompala G, Szutorisz H, Hurd YL (2021): Cannabis and synaptic reprogramming of the developing brain. Nat Rev Neurosci 22:423–438.
14. Katona I, Rancz EA, Acsady L, Ledent C, Mackie K, Hajos N, Freund TF (2001): Distribution of CB1 cannabinoid receptors in the amygdala and their role in the control of GABAergic transmission. J Neurosci 21:9506–9518.
15. Pine DS, Wise SP, Murray EA (2021): Evolution, emotion, and episodic engagement. Am J Psychiatry 178:701–714.
16. Petrovich GD, Canteras NS, Swanson LW (2001): Combinatorial amygdalar inputs to hippocampal domains and hypothalamic behavior systems. Brain Res Brain Res Rev 38:247–289.
17. Wassum KM, Izquierdo A (2015): The basolateral amygdala in reward learning and addiction. Neurosci Biobehav Rev 57:271–283.
18. Janak PH, Tye KM (2015): From circuits to behaviour in the amygdala. Nature 517:284–292.
19. Roy AK, Fudge JL, Kelly C, Perry JSA, Daniele T, Carlisi C, *et al.* (2013): Intrinsic functional connectivity of amygdala-based networks in adolescent generalized anxiety disorder. J Am Acad Child Adolesc Psychiatry 52:290–299.e2.
20. Hamilton JP, Siemer M, Gotlib IH (2008): Amygdala volume in major depressive disorder: A meta-analysis of magnetic resonance imaging studies. Mol Psychiatry 13:993–1000.
21. Jalbrzikowski M, Murty VP, Tervo-Clemmens B, Foran W, Luna B (2019): Age-associated deviations of amygdala functional connectivity in youths with psychosis spectrum disorders: Relevance to psychotic symptoms. Am J Psychiatry 176:196–207.
22. Spechler PA, Orr CA, Chaarani B, Kan KJ, Mackey S, Morton A, *et al.* (2015): Cannabis use in early adolescence: Evidence of amygdala hypersensitivity to signals of threat. Dev Cogn Neurosci 16:63–70.

23. Withey SL, Bergman J, Huestis MA, George SR, Madras BK (2020): THC and CBD blood and brain concentrations following daily administration to adolescent primates. Drug Alcohol Depend 213:108129.
24. Grotenhermen F (2003): Pharmacokinetics and pharmacodynamics of cannabinoids. Clin Pharmacokinet 42:327–360.
25. Manthey J, Freeman TP, Kilian C, López-Pelayo H, Rehm J (2021): Public health monitoring of cannabis use in Europe: Prevalence of use, cannabis potency, and treatment rates. Lancet Reg Health Eur 10:100227.
26. Linares IM, Zuardi AW, Pereira LC, Queiroz RH, Mechoulam R, Guimarães FS, Crippa JA (2019): Cannabidiol presents an inverted U-shaped dose-response curve in a simulated public speaking test. Braz J Psychiatry 41:9–14.
27. Jacobs DS, Kohut SJ, Jiang S, Nikas SP, Makriyannis A, Bergman J (2016): Acute and chronic effects of cannabidiol on Delta(9)-tetrahydrocannabinol Δ^9-tetrahydrocannabinol (Δ^9-THC)-induced disruption in stop signal task performance. Exp Clin Psychopharmacol 24:320–330.
28. Hindocha C, Freeman TP, Schafer G, Gardener C, Das RK, Morgan CJA, Curran HV (2015): Acute effects of delta-9-tetrahydrocannabinol, cannabidiol and their combination on facial emotion recognition: A randomised, double-blind, placebo-controlled study in cannabis users. Eur Neuropsychopharmacol 25:325–334.
29. Miller I, Scheffer IE, Gunning B, Sanchez-Carpintero R, Gil-Nagel A, Perry MS, *et al.* (2020): Dose-ranging effect of adjunctive oral cannabidiol vs placebo on convulsive seizure frequency in Dravet syndrome: A randomized clinical trial. JAMA Neurol 77:613–621.
30. Lust CAC, Lin X, Rock EM, Limebeer CL, Parker LA, Ma DWL (2022): Short communication: Tissue distribution of major cannabinoids following intraperitoneal injection in male rats. PLOS One 17:e0262633.
31. Spindle TR, Cone EJ, Schlienz NJ, Mitchell JM, Bigelow GE, Flegel R, *et al.* (2018): Acute effects of smoked and vaporized cannabis in healthy adults who infrequently use cannabis: A crossover trial. JAMA Netw Open 1:e184841.
32. Gelmi TJ, Weinmann W, Pfäffli M (2021): Impact of smoking cannabidiol (CBD)-rich marijuana on driving ability. Forensic Sci Res 6:195–207.
33. Shumyatsky GP, Malleret G, Shin RM, Takizawa S, Tully K, Tsvetkov E, *et al.* (2005): stathmin, a gene enriched in the amygdala, controls both learned and innate fear. Cell 123:697–709.
34. Uchida S, Martel G, Pavlowsky A, Takizawa S, Hevi C, Watanabe Y, *et al.* (2014): Learning-induced and stathmin-dependent changes in microtubule stability are critical for memory and disrupted in ageing. Nat Commun 5:4389.
35. Mohan V, Gomez JR, Maness PF (2019): Expression and function of neuron-glia-related cell adhesion molecule (NrCAM) in the amygdalar pathway. Front Cell Dev Biol 7:9.
36. Takano T, Wallace JT, Baldwin KT, Purkey AM, Uezu A, Courtland JL, *et al.* (2020): Chemico-genetic discovery of astrocytic control of inhibition in vivo. Nature 588:296–302.
37. Pekny M, Pekna M (2014): Astrocyte reactivity and reactive astrogliosis: Costs and benefits. Physiol Rev 94:1077–1098.
38. Yong VW, Moumdjian R, Yong FP, Ruijs TC, Freedman MS, Cashman N, Antel JP (1991): Gamma-interferon promotes proliferation of adult human astrocytes in vitro and reactive gliosis in the adult mouse brain in vivo. Proc Natl Acad Sci USA 88:7016–7020.
39. Withey SL, Kangas BD, Charles S, Gumbert AB, Eisold JE, George SR, *et al.* (2021): Effects of daily Δ9-tetrahydrocannabinol (THC) alone or combined with cannabidiol (CBD) on cognition-based behavior and activity in adolescent nonhuman primates. Drug Alcohol Depend 221:108629.
40. Di Raddo ME, Milenkovic M, Sivasubramanian M, Hasbi A, Bergman J, Withey S, *et al.* (2023): Δ9-tetrahydrocannabinol does not upregulate an aversive dopamine receptor mechanism in adolescent brain unlike in adults. Curr Res Neurobiol 5:100107.
41. Sosunov A, Wu XP, McGovern R, Mikell C, McKhann GM, Goldman JE (2020): Abnormal mitosis in reactive astrocytes. Acta Neuropathol Commun 8:47.
42. Cerutti SM, Chadi G (2000): S100 immunoreactivity is increased in reactive astrocytes of the visual pathways following a mechanical lesion of the rat occipital cortex. Cell Biol Int 24:35–49.
43. Lian H, Yang L, Cole A, Sun L, Chiang ACA, Fowler SW, *et al.* (2015): NFκB-activated astroglial Release of Complement C3 Compromises Neuronal Morphology and Function Associated with Alzheimer's disease. Neuron 85:101–115.
44. Ferland JN, Ellis RJ, Rompala G, Landry JA, Callens JE, Ly A, *et al.* (2023): Dose mediates the protracted effects of adolescent THC exposure on reward and stress reactivity in males relevant to perturbation of the basolateral amygdala transcriptome. Mol Psychiatry 28:2583–2593.
45. Boutej H, Rahimian R, Thammisetty SS, Béland LC, Lalancette-Hébert M, Kriz J (2017): Diverging mRNA and protein networks in activated microglia reveal SRSF3 suppresses translation of highly upregulated innate immune transcripts. Cell Rep 21:3220–3233.
46. Zamberletti E, Gabaglio M, Grilli M, Prini P, Catanese A, Pittaluga A, *et al.* (2016): Long-term hippocampal glutamate synapse and astrocyte dysfunctions underlying the altered phenotype induced by adolescent THC treatment in male rats. Pharmacol Res 111:459–470.
47. Suárez I, Bodega G, Fernández-Ruiz JJ, Ramos JA, Rubio M, Fernández B (2002): Reduced glial fibrillary acidic protein and glutamine synthetase expression in astrocytes and Bergmann glial cells in the rat cerebellum caused by delta(9)-tetrahydrocannabinol administration during development. Dev Neurosci 24:300–312.
48. Suárez I, Bodega G, Ramos JA, Fernández-Ruiz JJ, Fernández B (2000): Neuronal and astroglial response to pre- and perinatal exposure to delta-9-tetra- hydrocannabinol in the rat substantia nigra. Dev Neurosci 22:253–263.
49. Stevens B, Allen NJ, Vazquez LE, Howell GR, Christopherson KS, Nouri N, *et al.* (2007): The classical complement cascade mediates CNS synapse elimination. Cell 131:1164–1178.
50. VanRyzin JW, Marquardt AE, Argue KJ, Vecchiarelli HA, Ashton SE, Arambula SE, *et al.* (2019): Microglial phagocytosis of newborn cells is induced by endocannabinoids and sculpts sex differences in juvenile rat social play. Neuron 102:435–449.e6.
51. Sellgren CM, Gracias J, Watmuff B, Biag JD, Thanos JM, Whittredge PB, *et al.* (2019): Increased synapse elimination by microglia in schizophrenia patient-derived models of synaptic pruning. Nat Neurosci 22:374–385.
52. Carlstrom EL, Niazi A, Etemadikhah M, Halvardson J, Enroth S, Stockmeier CA, *et al.* (2021): Transcriptome analysis of post-mortem brain tissue reveals up-regulation of the complement cascade in a subgroup of schizophrenia patients. Genes (Basel) 12:1242.
53. Wei JX, Liu Y, Zhao LS, Yang X, Ni PY, Wang YC, *et al.* (2018): Plasma complement component 4 increases in patients with major depressive disorder. Neuropsychiatr Dis Treat 14:37–41.
54. Costello H, Gould RL, Abrol E, Howard R (2019): Systematic review and meta-analysis of the association between peripheral inflammatory cytokines and generalised anxiety disorder. BMJ Open 9:e027925.
55. Freeman D, Sheaves B, Waite F, Harvey AG, Harrison PJ (2020): Sleep disturbance and psychiatric disorders. Lancet Psychiatry 7:628–637.
56. Coelho J, Montagni I, Micoulaud-Franchi JA, Plancoulaine S, Tzourio C (2023): Study of the association between cannabis use and sleep disturbances in a large sample of University students. Psychiatry Res 322:115096.
57. Brancaccio M, Edwards MD, Patton AP, Smyllie NJ, Chesham JE, Maywood ES, Hastings MH (2019): Cell-autonomous clock of astrocytes drives circadian behavior in mammals. Science 363:187–192.
58. Halassa MM, Florian C, Fellin T, Munoz JR, Lee SY, Abel T, *et al.* (2009): Astrocytic modulation of sleep homeostasis and cognitive consequences of sleep loss. Neuron 61:213–219.
59. Pocivavsek A, Baratta AM, Mong JA, Viechweg SS (2017): Acute kynurenine challenge disrupts sleep-wake architecture and impairs contextual memory in adult rats. Sleep 40:zsx141.
60. Ingiosi AM, Hayworth CR, Harvey DO, Singletary KG, Rempe MJ, Wisor JP, Frank MG (2020): A role for astroglial calcium in mammalian sleep and sleep regulation. Curr Biol 30:4373–4383.e7.
61. Feneberg E, Steinacker P, Lehnert S, Böhm B, Mayer G, Otto M (2013): Elevated glial fibrillary acidic protein levels in the cerebrospinal fluid of patients with narcolepsy. Sleep Med 14:692–694.

62. Cho HJ, Savitz J, Dantzer R, Teague TK, Drevets WC, Irwin MR (2017): Sleep disturbance and kynurenine metabolism in depression. J Psychosom Res 99:1–7.
63. Moy SS, Nonneman RJ, Young NB, Demyanenko GP, Maness PF (2009): Impaired sociability and cognitive function in Nrcam-null mice. Behav Brain Res 205:123–131.
64. Ishiguro H, Liu QR, Gong JP, Hall FS, Ujike H, Morales M, *et al.* (2006): NrCAM in addiction vulnerability: Positional cloning, drug-regulation, haplotype-specific expression, and altered drug reward in knockout mice. Neuropsychopharmacology 31:572–584.
65. Morgan CJA, Freeman TP, Schafer GL, Curran HV (2010): Cannabidiol attenuates the appetitive effects of Delta9-tetrahydrocannabinol in humans smoking their chosen cannabis. Neuropsychopharmacology 35:1879–1885.
66. Taffe MA, Creehan KM, Vandewater SA (2015): Cannabidiol fails to reverse hypothermia or locomotor suppression induced by Δ(9) -tetrahydrocannabinol in Sprague-Dawley rats. Br J Pharmacol 172:1783–1791.
67. Laprairie RB, Bagher AM, Kelly MEM, Denovan-Wright EM (2015): Cannabidiol is a negative allosteric modulator of the cannabinoid CB1 receptor. Br J Pharmacol 172:4790–4805.
68. Scarante FF, Ribeiro MA, Almeida-Santos AF, Guimarães FS, Campos AC (2020): Glial cells and their contribution to the mechanisms of action of cannabidiol in neuropsychiatric disorders. Front Pharmacol 11:618065.
69. Hind WH, England TJ, O'Sullivan SE (2016): Cannabidiol protects an in vitro model of the blood-brain barrier from oxygen-glucose deprivation via PPARgamma and 5-HT1A receptors. Br J Pharmacol 173:815–825.
70. Boddum K, Jensen TP, Magloire V, Kristiansen U, Rusakov DA, Pavlov I, Walker MC (2016): Astrocytic GABA transporter activity modulates excitatory neurotransmission. Nat Commun 7:13572.
71. Semyanov A, Henneberger C, Agarwal A (2020): Making sense of astrocytic calcium signals – From acquisition to interpretation. Nat Rev Neurosci 21:551–564.
72. Martin-Fernandez M, Jamison S, Robin LM, Zhao Z, Martin ED, Aguilar J, *et al.* (2017): Synapse-specific astrocyte gating of amygdala-related behavior. Nat Neurosci 20:1540–1548+.
73. Chen RQ, Zhang J, Fan N, Teng ZQ, Wu Y, Yang HW, *et al.* (2013): Δ9-THC-caused synaptic and memory impairments are mediated through COX-2 signaling. Cell 155:1154–1165.
74. Lauckner JE, Hille B, Mackie K (2005): The cannabinoid agonist WIN55,212-2 increases intracellular calcium via CB1 receptor coupling to Gq/11 G proteins. Proc Natl Acad Sci USA 102:19144–19149.
75. Zeng W, Mak DOD, Li Q, Shin DM, Foskett JK, Muallem S (2003): A new mode of Ca2+ signaling by G protein-coupled receptors: Gating of IP3 receptor Ca2+ release channels by Gbetagamma. Curr Biol 13:872–876.
76. Long LE, Lind J, Webster M, Weickert CS (2012): Developmental trajectory of the endocannabinoid system in human dorsolateral prefrontal cortex. BMC Neurosci 13:87.
77. Zhang LY, Kim AY, Cheer JF (2022): Regulation of glutamate homeostasis in the nucleus accumbens by astrocytic CB1 receptors and its role in cocaine-motivated behaviors. Addict Neurosci 3:100022.